Supporting information for:

Kinetic Stability-driven Cytotoxicity of Small-molecule Prodrug Nanoassemblies

Yang Li[a], Yuwen Chen[a], Yulan Huang[a], Wengbi Wu[a], Yu Liu[a], Jing Zhang[b], Meijuan Huang [c], Maling Gou[a]*

[a]State Key Laboratory of Biotherapy and Cancer Center, West China Hospital, Sichuan University, Chengdu, 610041, China.

[b]Department of Neurosurgery, West China Hospital, Sichuan University, Chengdu 610041, China.

[c] Department of Thoracic Oncology, Cancer Center, West China Hospital, Medical School, Sichuan University, Chengdu, 610041, China.

*Corresponding author: Maling Gou (goumaling@scu.edu.cn)

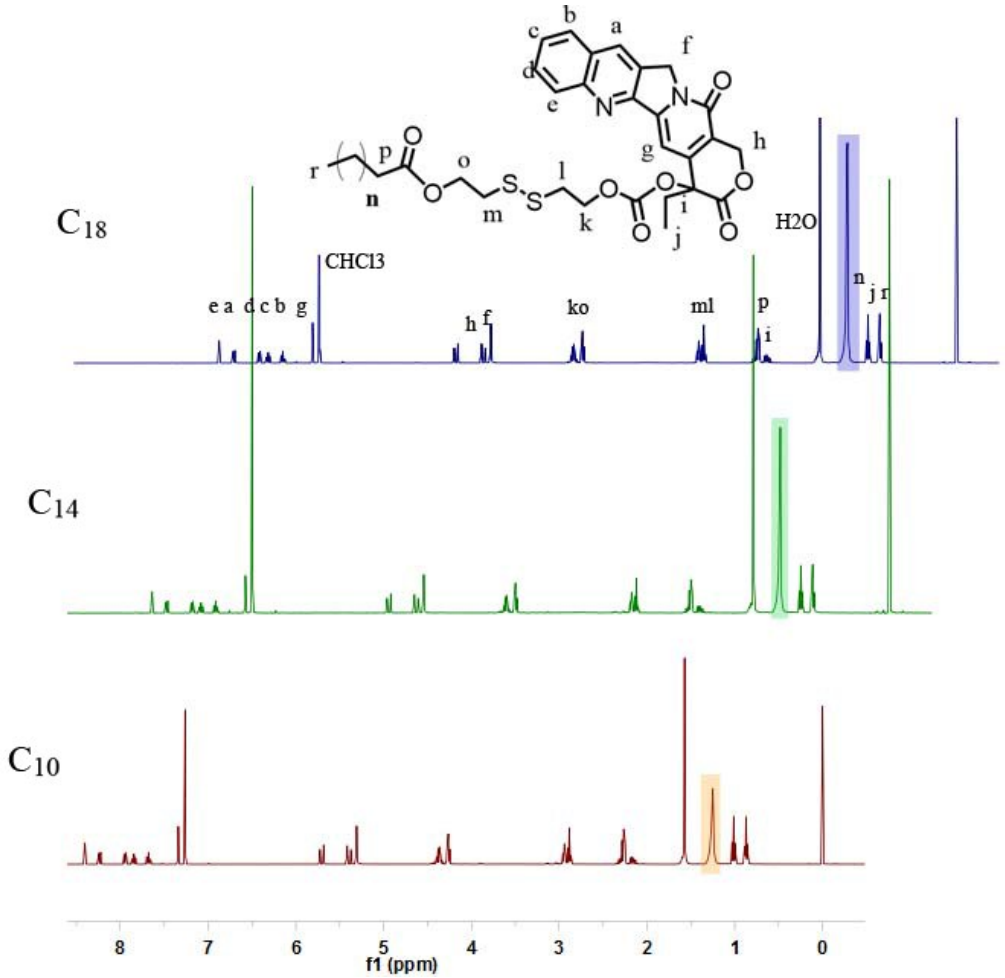

Figure.S1 H[1]-NMR of etcSS-linked lipophilic CPT prodrugs with different chain lengths (C_{10}, C_{14} and C_{18}).

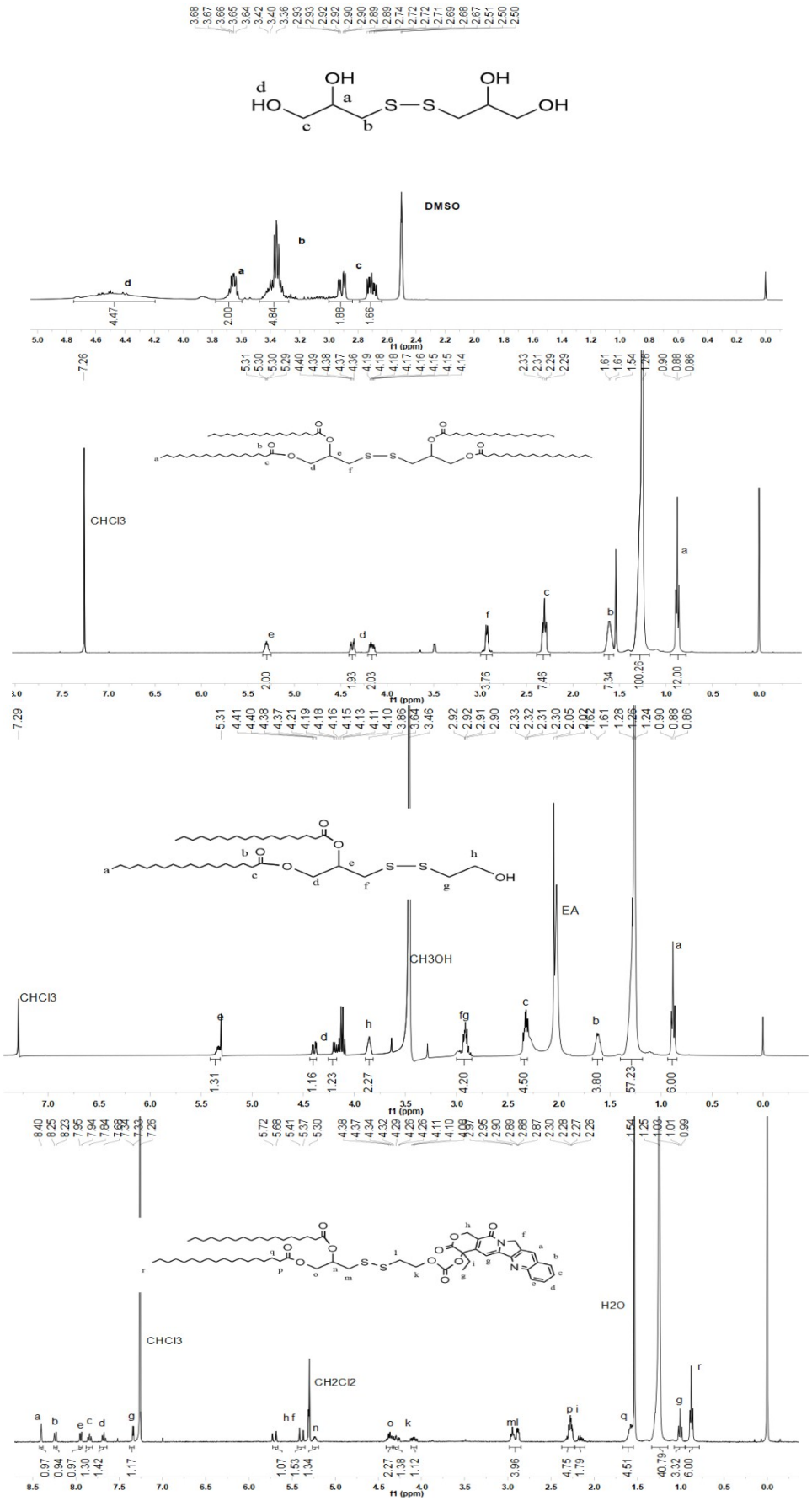

Figure.S2 H^1-NMR of CPT-etcSS-$2C_{18}$ and related synthetic intermediates (Product 1, Product 2, Product 3)

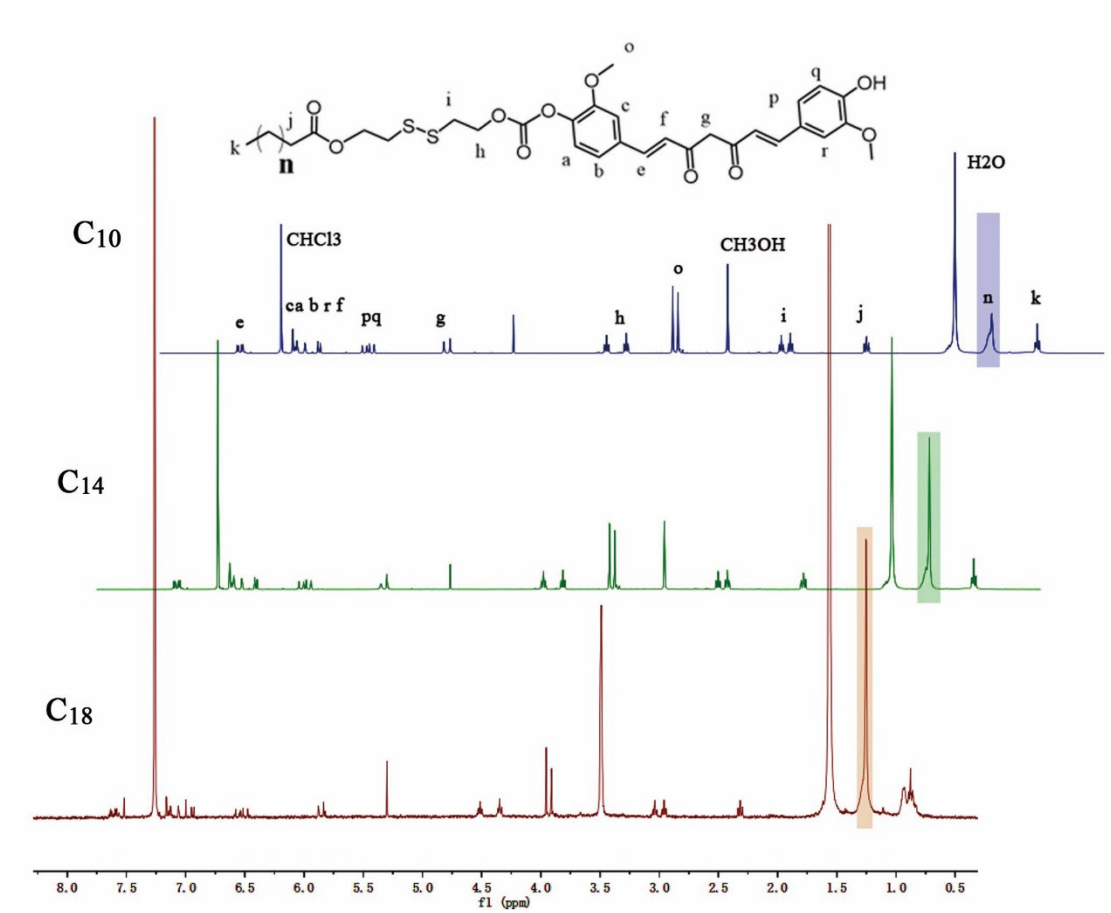

Figure.S3 H^1-NMR of etcSS-linked lipophilic CUR prodrug with different chain lengths (C_{10}, C_{14} and C_{18})

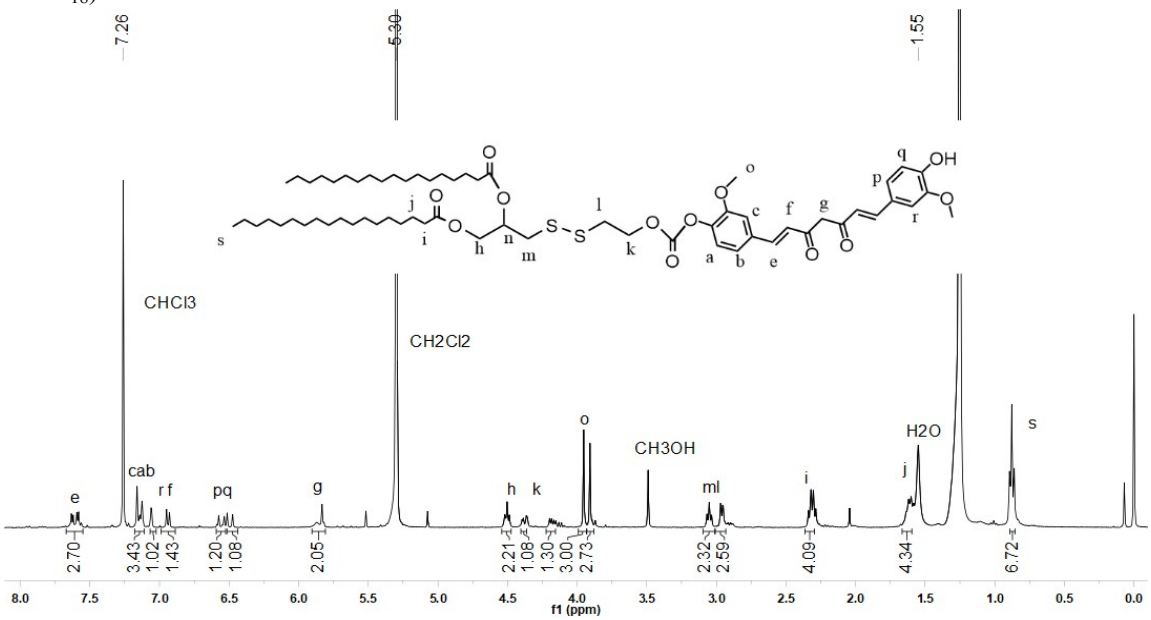

Figure.S4 H^1-NMR of CUR-etcSS-2C_{18}

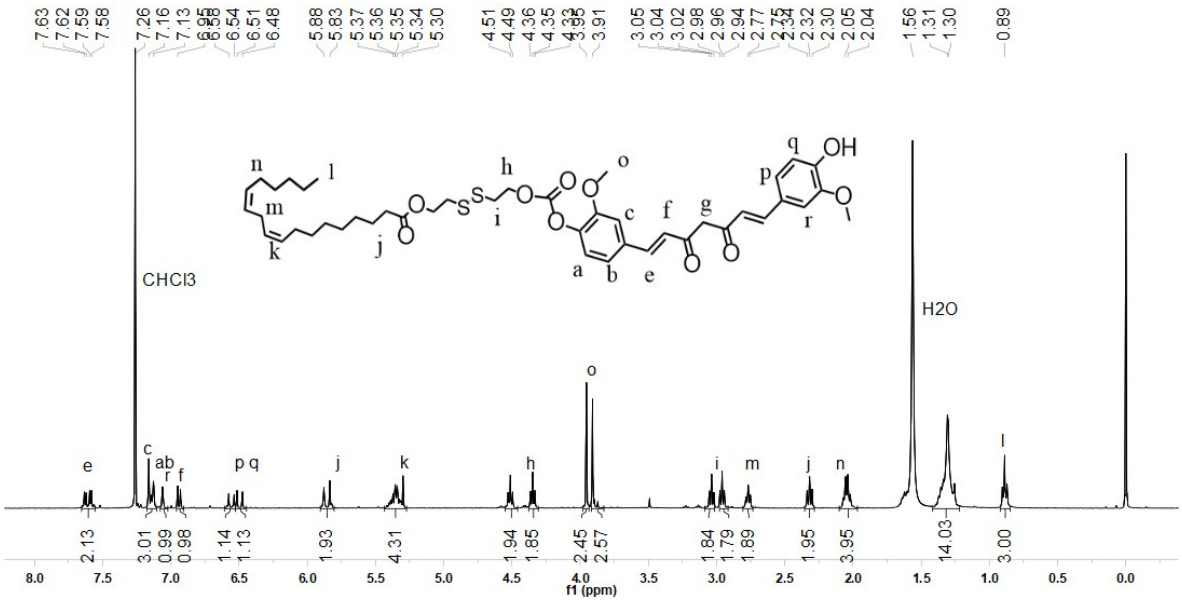

Figure.S5 H^1-NMR of CUR-etcSS-$C_{18:2}$

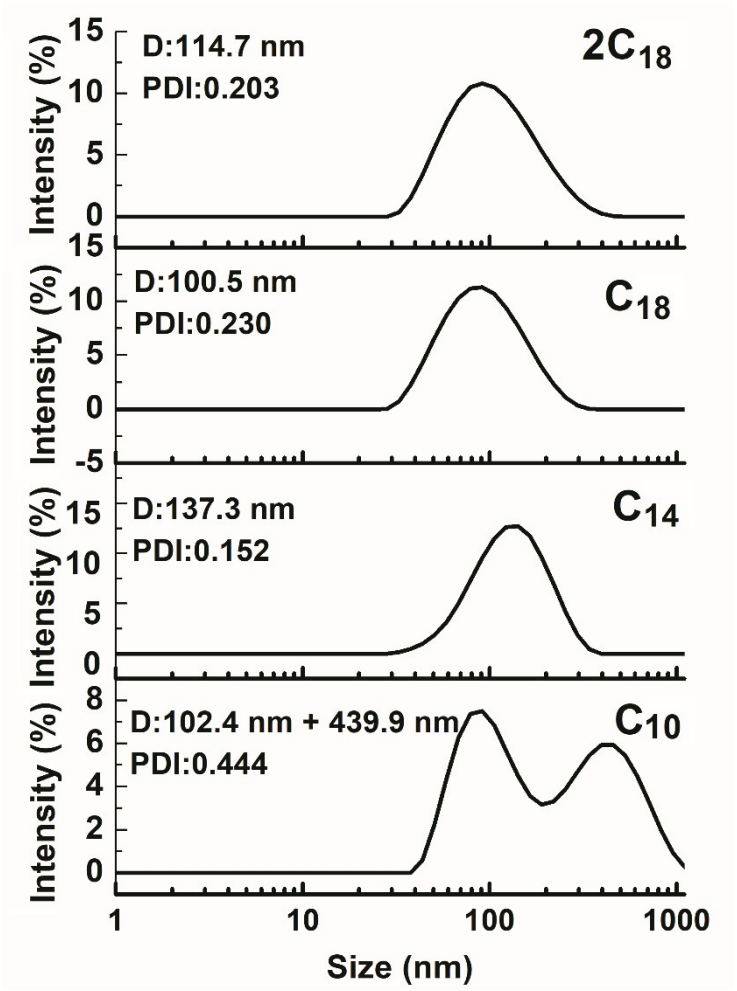

Figure.S6 Size distributions of the CPT-CUR-NAs of C_{10}, C_{14}, C_{18} and $2C_{18}$

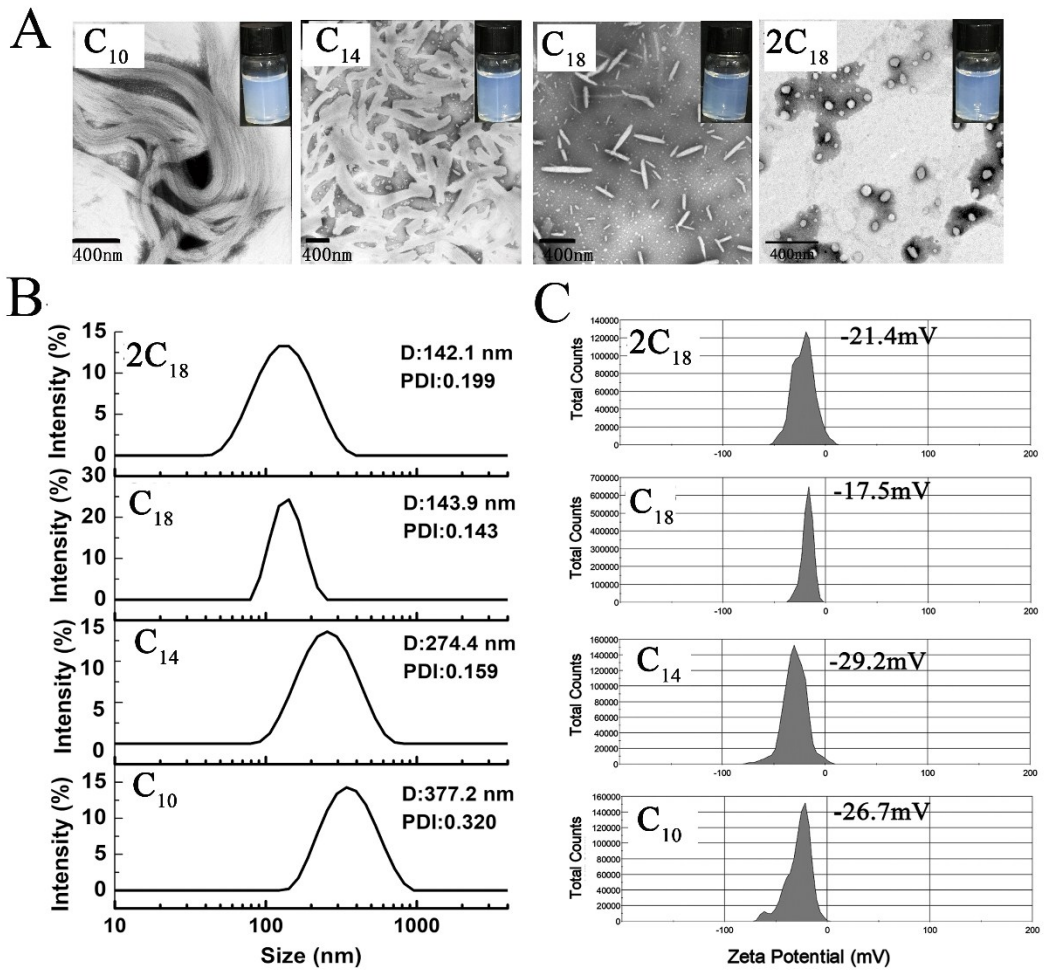

Figure.S7 Lipophilic prodrug of CPT co-assembled with DSPE-mPEG$_{2000}$ to form various well-ordered nanostructures (C_{10}, nanofiber; C_{14}, nanoribbon; C_{18}, nanorod; $2C_{18}$, nanosphere) (A). The size distributions (B) and zeta potentials (C) of the CPT-NAs of C_{10}, C_{14}, C_{18} and $2C_{18}$

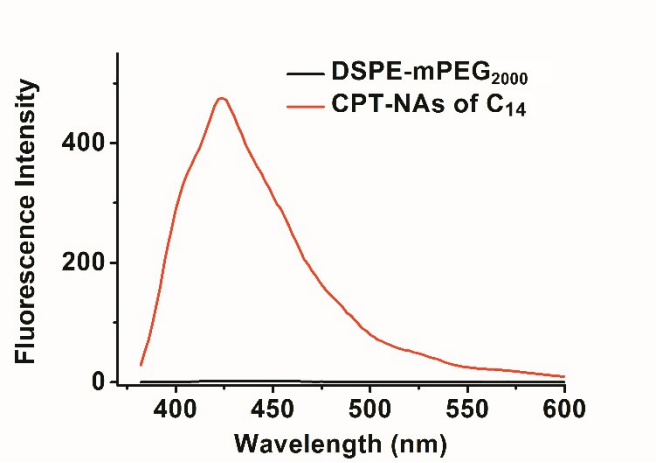

Figure.S8 Emission spectra of CPT-NAs of C_{14} and DSPE-mPEG$_{2000}$

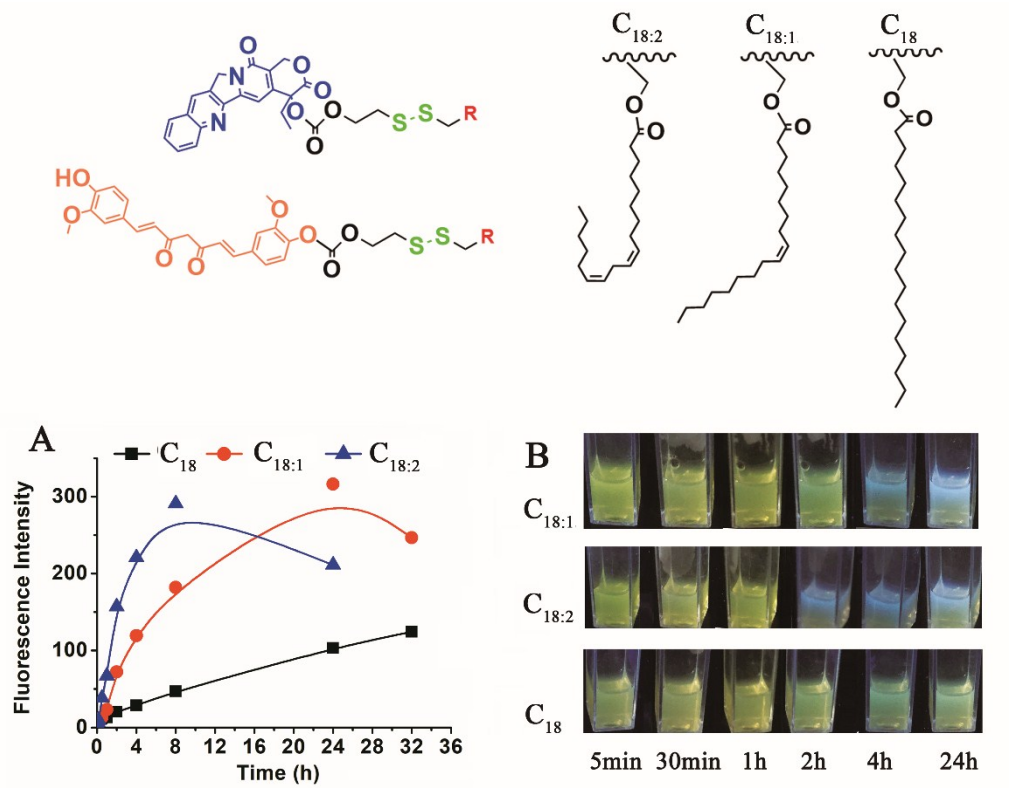

Figure.S9 Kinetic changes of emission fluorescence intensity at 426 nm (A) and picture under a UV lamp (B) of CPT-CUR-NAs of C_{18}, $C_{18:1}$ and $C_{18:2}$ upon incubation with blank liposomes (2.5 mg/ml) at 37.5 °C.

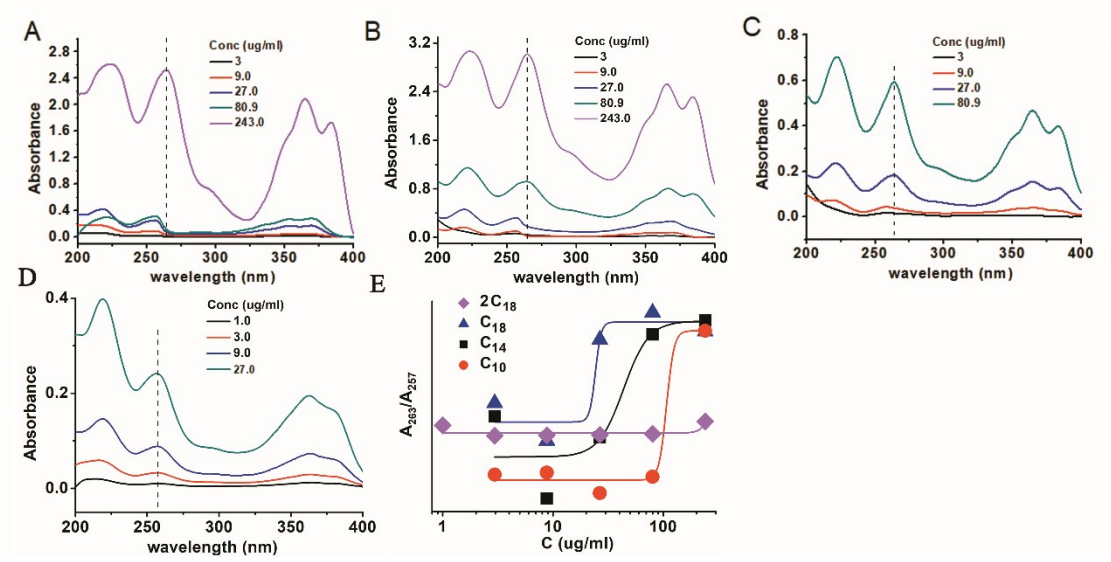

Figure.S10 Evaluation of thermodynamic stability of CPT-NAs of C_{10} (A), C_{14} (B), C_{18} (C) and $2C_{18}$ (D) by measuring their UV-vis spectra at various concentrations in the 50 % ethanol solution at 25 °C. The critical aggregation concentration was evaluated according to the change of intensity ratio (I_{263}/I_{257}) versus the concentration of CPT-NAs (E).

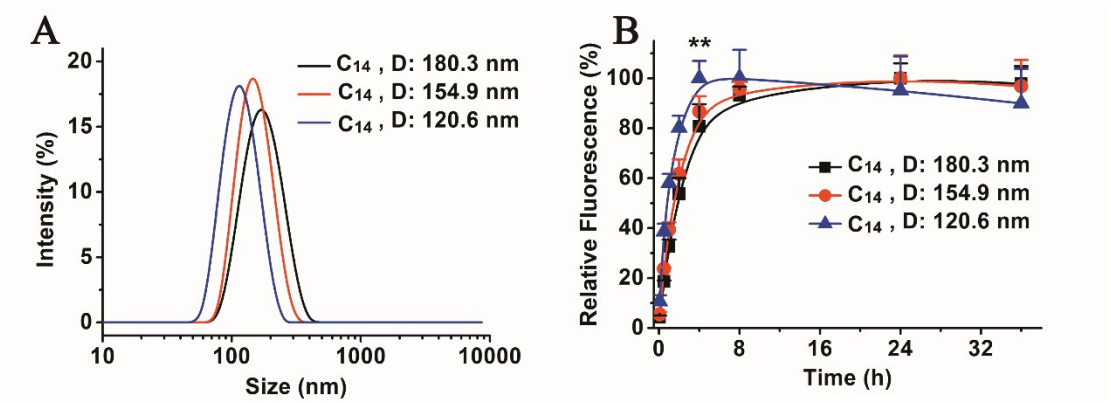

Figure.S11 Size distributions of CPT-CUR-NAs of C_{14} prepared by dispersing ethanol solution of lipophilic prodrug of CPT and CUR with various concentrations (i.e. 5, 10 and 20 mg/ml) into distilled water (A). Kinetic changes of emission fluorescence intensity at 426 nm (expressed as percentages of the maximum fluorescence, [means ± SD, n = 4], **p< 0.01 at 4 h) of these CPT-CUR-NAs upon incubation with blank liposomes (2.5 mg/ml) at 37.5 °C (B).

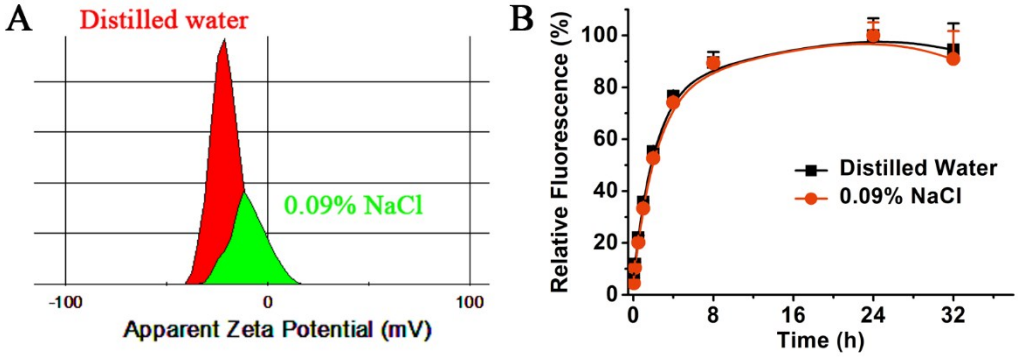

Figure.S12 Zeta potentials of CPT-CUR-NAs of C_{14} in distilled water and 0.09 % NaCl solution (A). Kinetic changes of fluorescence intensity at 426 nm of CPT-CUR-NAs upon incubation with blank liposomes (2.5 mg/ml) in distilled water and 0.09 % NaCl solution at 37.5 °C, [means ± SD, n = 4].

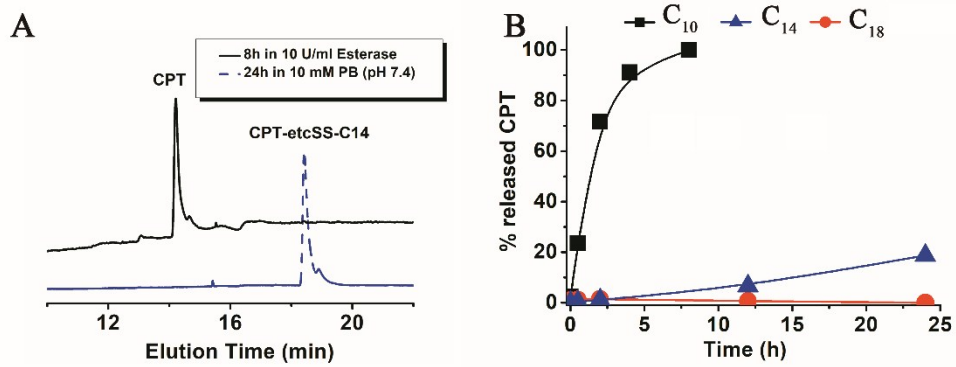

Figure.S13 HPLC analysis of CPT-NAs of C_{10} after incubation in the 10 mM PB (pH 7.4, 24 h) and 10 U/ml porcine liver esterase (model esterase, 8 h) (A). *In vitro* release profiles of CPT from CPT-NAs of C_{10}, C_{14} and C_{18} in the 10 U/ml esterase at 37.5 °C (B).

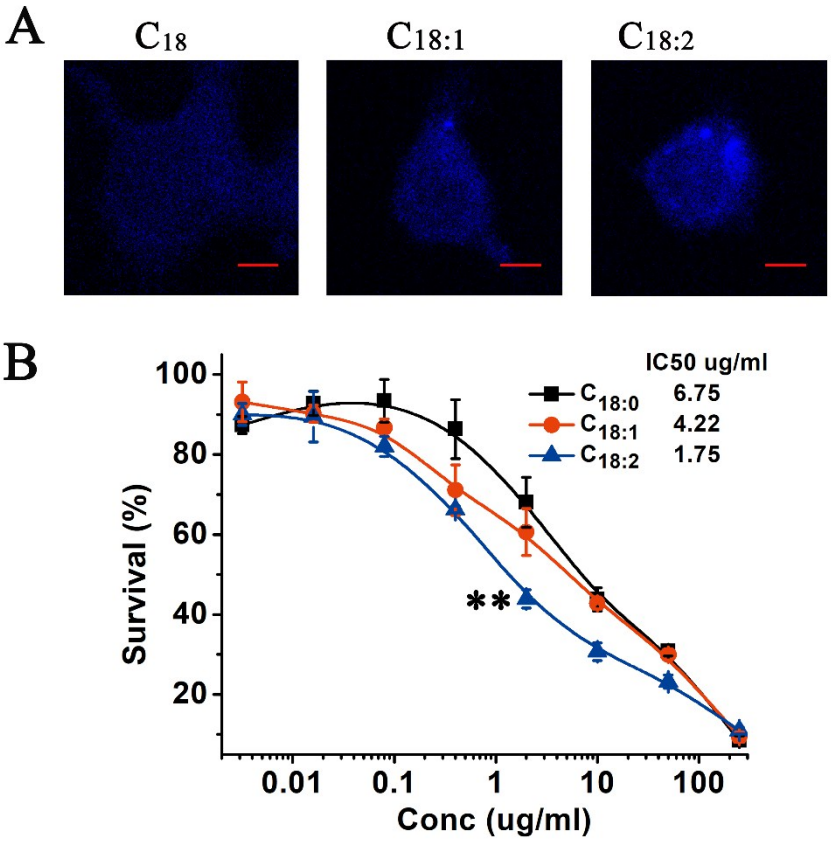

Figure.S14 Real-time visualization of intracellular disassembly of CPT-NAs of C_{18}, $C_{18:1}$ and $C_{18:2}$ in the CT26 cells detected by a confocal microscope (A). Cytotoxicity of CPT-NAs of C_{18}, $C_{18:1}$ and $C_{18:2}$ against the CT26 determined by the MTT assay, [means±SD, n = 4], **p < 0.01 at 2 μg/ml (B).